Modeling Current Distributions in Short-Sample Rutherford Cables Under Self-field Conditions

Jason McDonald

Abstract:

Simulations were performed on an electrical-network model for Rutherford-type cables, to study the predicted current distributions in a short sample subjected to a current ramp. The dependence of the current distribution on various parameters is presented and discussed, including implications for recent measurements performed at Fermilab.

Introduction:

Recent measurements performed at Fermilab [1, 2] have shown that short cable samples, measured under self-field conditions, can have critical current degradations of 80% or more compared to expectations from measurements on individual strands. The source of this degradation has not yet been identified, but there has been some speculation that large current imbalances may play a role [3].

The purpose of the present work is to model a Rutherford cable exposed to a ramped current, and to determine how the current distributions depend on the various parameters. The calculations were performed on an electrical-network model [4], which has been modified so that all inductive interactions can be efficiently incorporated [5]. The accurate treatment of all inductive interactions is imperative under self-field conditions, because transposition does little to reduce inductive couplings in this case [6].

Problem Description:

Consider a 28-strand cable having a transposition-pitch length L_p (see Figure 1). For the calculations in this paper we will consider a cable of length $5L_p$, since this is a typical length used in the measurements [1, 2]. The cable is modeled as a collection of 3-dimensional circuits consisting of sections of strand and contact resistances [4, 5]. Each strand section is represented by a resistance and a self inductance, and each pair of strand sections is linked by a mutual inductance. The contact resistances fall into two categories: electrical contacts between strands in the same layer are called adjacent contacts and are labeled R_a, while contacts between strands in different layers are called crossover contacts and are labeled R_c. The values of the self inductances depend on both the length and diameter of the strand sections [7]; as a general rule the self-inductance values increase with length and decrease with diameter.

In the experiments the ends of the cable are soldered over a length of L_p. In order to represent the soldered connections in the calculations, the values of $R_a = R_c = 30\ n\Omega$ were used, which are consistent with the measured splice resistance.

Results:

A systematic study was performed to determine the dependence of the current distribution upon various parameters. For purposes of display, the strands were numbered as shown in Figure 2.

Dependence on ramprate of current:

A series of simulations were performed for current ramprates of 50, 100, 200 and 400 Amps / sec, the values of all other parameters being fixed. The results of the simulations are displayed in Figures 3, 4, and 5. It is clear from the results that there is a small current imbalance which becomes more pronounced as the ramprate is increased, and that the current imbalance penetrates all the way through a short cable.

Dependence on strand resistivity:

A series of simulations were performed for strand resistivities of zero, 10^{-16}, 10^{-15}, and $10^{-14} \, \Omega \cdot m$, the values of all other parameters being fixed. The results are displayed in Figure 6. It is clear that the current imbalance begins increasing with decreasing ρ_s, but that it saturates once ρ_s gets much below $10^{-14} \, \Omega \cdot m$. Calculations were also performed on a longer cable (total length of $20L_p$ instead of $5L_p$) to determine how the current-imbalance pattern decays away from the soldered region. The results are displayed in Figures 7 and 8. It can be seen from the figures that the decay length gradually increases with decreasing ρ_s. As in the case of Boundary-Induced Coupling Currents (BICCs) [4], for small ρ_s the current pattern can penetrate a great distance along the cable.

Dependence on contact resistance:

A series of simulations were performed for contact resistance values of 0.3, 3, and $30 \mu\Omega$, the values of all other parameters being fixed. The results are shown in Figures 8. It can be observed that the current imbalance becomes more pronounced for $R_a, R_c < 1 \, \mu\Omega$, but seems to quickly approach a limiting distribution for $R_a, R_c > 1 \, \mu\Omega$. Figures 4, 9, and 10 illustrate that the current distributions along the cable are greatly affected by the contact resistance values: the oscillatory pattern, with a period of $L_p / 2$, is more pronounced as the contact resistance value decreases, indicating that the pattern is due to coupling currents between strands; this oscillation is similar to what is observed in BICCs, but the period is smaller by a factor of 2.

Dependence on strand diameter:

Simulations were performed for strand diameter values of 0.5 and 1.0 *mm*, the values of all other parameters being fixed. The cable with $d_s = 0.5$ *mm* has about 30% higher self inductance per strand section than the cable with

$d_s = 1.0 \ mm$; since the strands are being approximated by wires, an increase in d_s does not affect the mutual inductance values [7]. The results are presented in Figure 12. It appears that a relatively large increase in self inductance does not lead to a significant increase in the current imbalance.

Effect of soldered ends:

If the regions at the ends of the cable are given the same contact resistance values as the central region, then the current imbalance disappears. This indicates that the imbalance is a boundary-induced effect which is caused by the changing self field in the presence of a discontinuity in contact resistance values.

Conclusion:

Simulations performed on a modified network model of a Rutherford cable [5] indicate that the soldered regions at the ends of a cable can cause boundary-induced currents in the presence of a changing self field. These boundary induced currents become more pronounced as the self-field ramprate is increased, but for realistic values they do not appear to cause significant current imbalances; therefore, the source of the premature quenches in recent short-sample tests [1, 2] remains an open question.

.

References:

[1]   G. Ambrosio, results presented at the *Workshop on Instabilities in Nb₃Sn Strands, Cables, and Magnets,* Fermilab, April 28-30, 2004.

[2]   D. Turrioni, results presented at the *Workshop on Instabilities in Nb₃Sn Strands, Cables, and Magnets,* Fermilab, April 28-30, 2004.

[3]   M. Wake, results presented at the *Workshop on Instabilities in Nb₃Sn Strands, Cables, and Magnets,* Fermilab, April 28-30, 2004.

[4]   A. P. Verweij, PhD Thesis, University of Twente, Enschede, Netherlands (1995).

[5]   J. McDonald, Fermilab Technical Documents: TD-04-017, TD-04-018 (2004).

[6]   M. N. Wilson, *Superconducting Magnets*, Oxford University Press, Oxford, England (1983).

[7]   F. W. Grover, *Inductance Calcuations*, Dover, New York, NY (1962).

Figures:
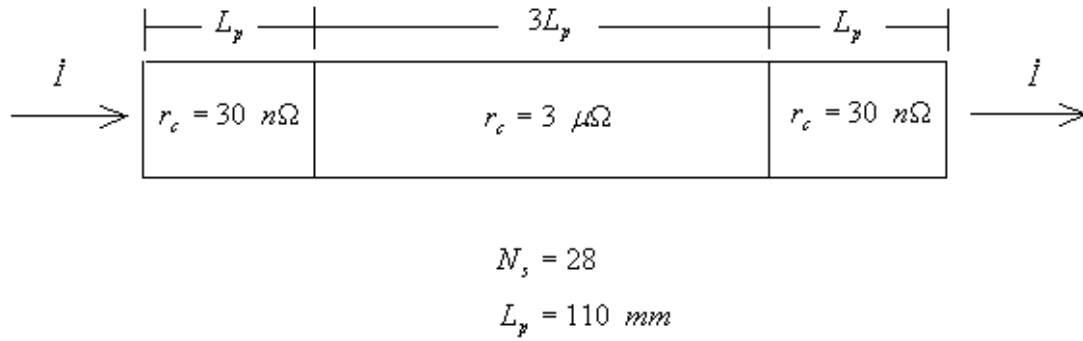
Figure 1   The geometry used in the calculations consists of a 28-strand cable of total length $5L_p$; a length of L_p on either end was modeled as a soldered connection with very small contact resistances. The values of the contact resistances, strand resistances, and strand diameters were varied in the central region to determine their effect on current distribution between strands. In addition, the dependence on the ramprate for the transport current was also investigated.
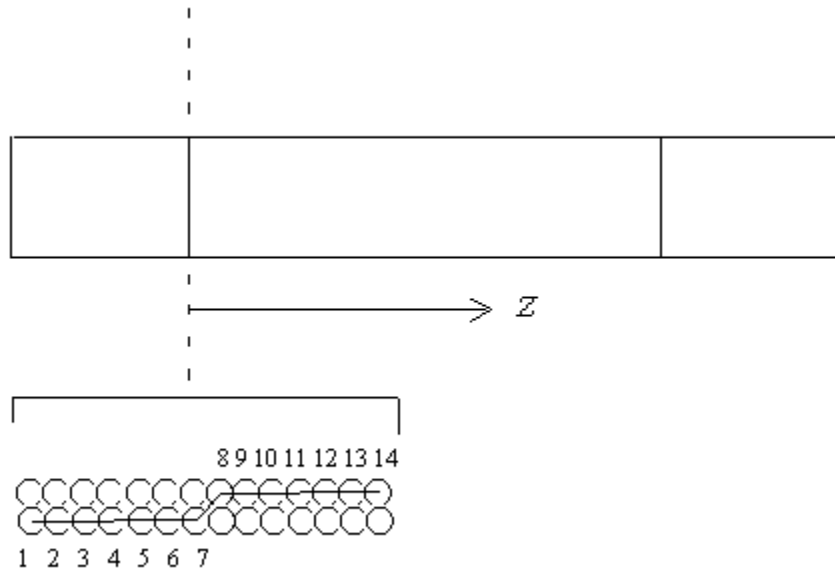
Figure 2   The strand numbering used in the plots of strand current. Strands   and 14
            wrap around the sides of the cable at the end of the first soldered region.
            The coordinate z labels the distance from the end of the first soldered
            region.
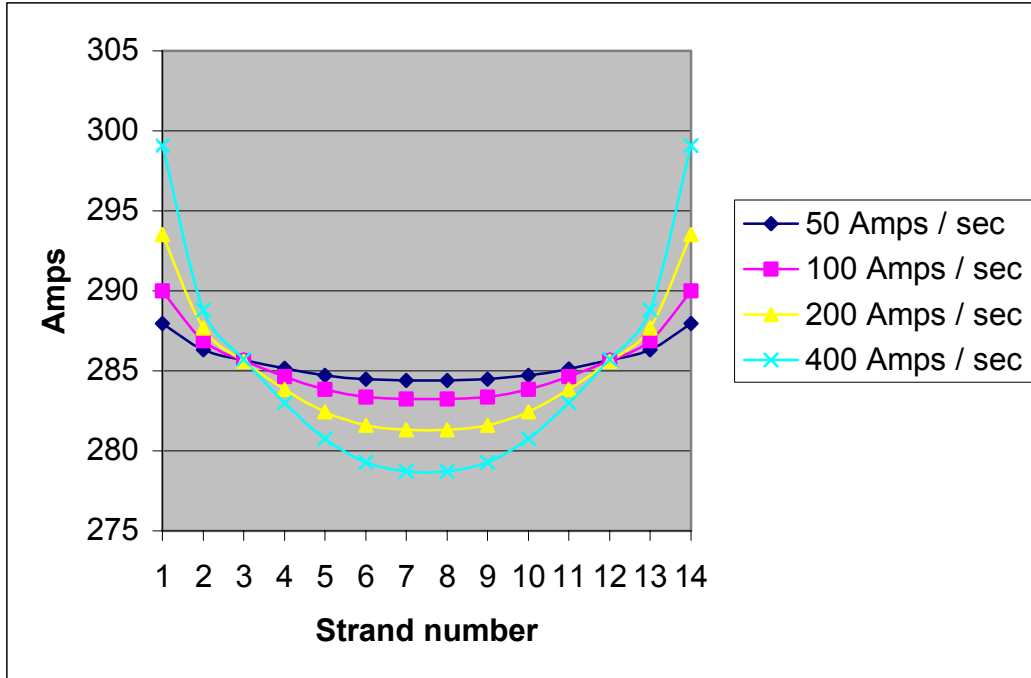
Figure 3   The distribution of strand currents, at the crossection $z = 0$, for four different values of current ramprate. The values used for the other parameters were: strand diameter $d_s = 1$ mm, strand resistivity $\rho_s = 10^{-14} \Omega \cdot m$, and $R_a = R_c = 3$ $\mu\Omega$. The expected value of strand current (if there was no imbalance) at this instant of time is 285.7 Amps.
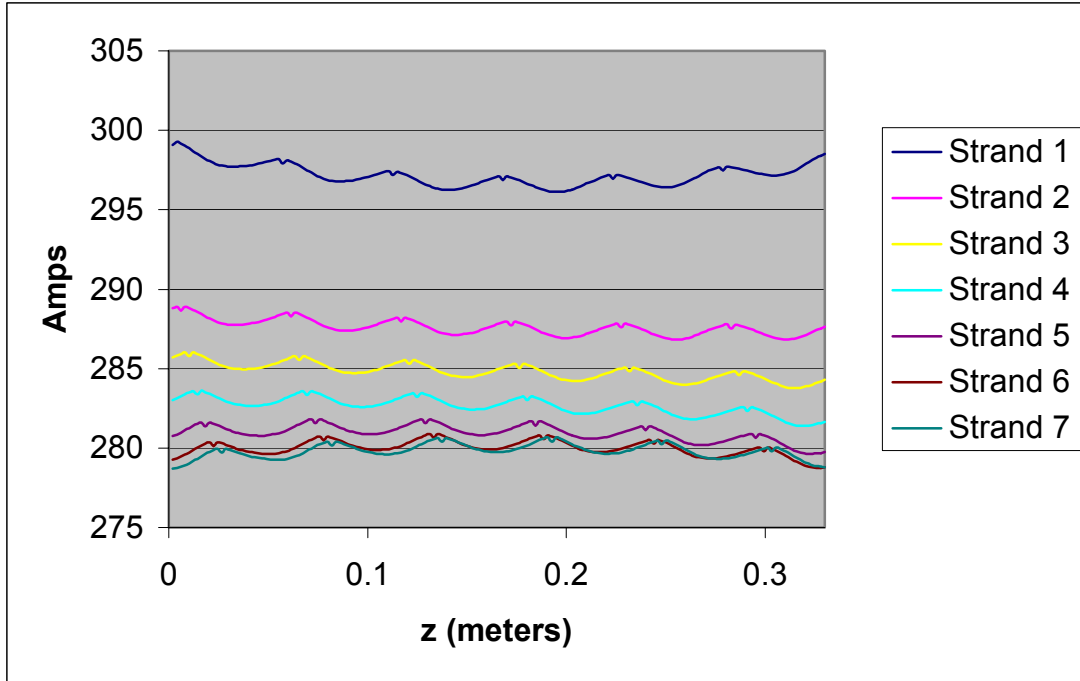
Figure 4   The distribution of strand currents along the cable length for a current ramprate of 400 Amps / sec, $d_s = 1 \ mm$, $\rho_s = 10^{-14} \Omega \cdot m$, and $R_a = R_c = 3 \ \mu\Omega$.
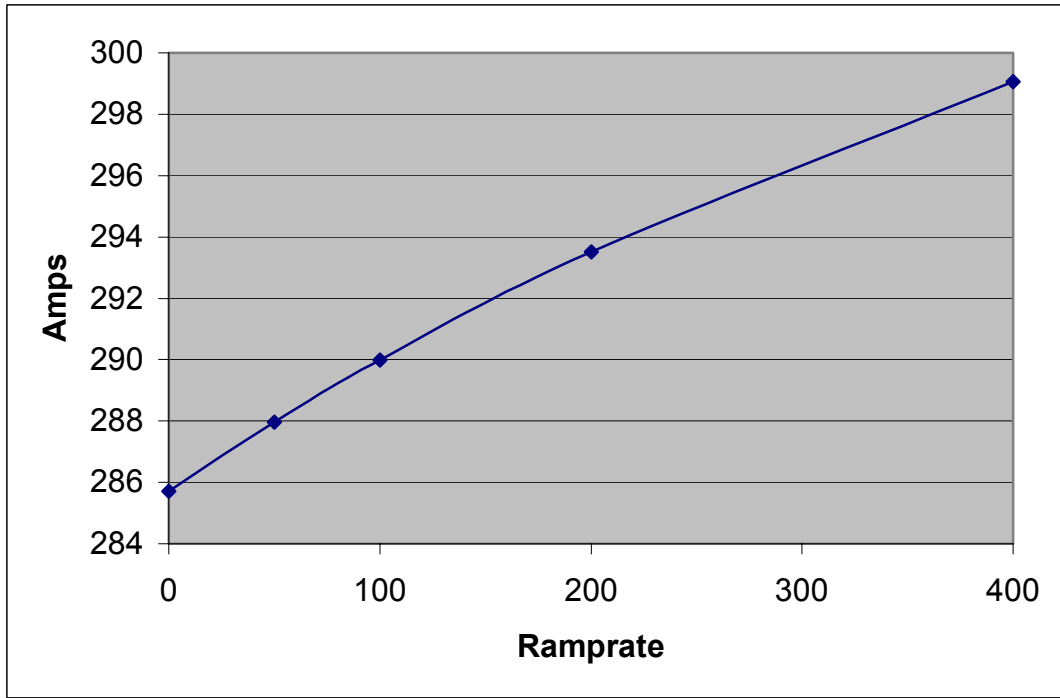
Figure 5　　Maximum strand current versus ramprate for the parameter values $d_s = 1\ mm$, $\rho_s = 10^{-14}\,\Omega \cdot m$, and $R_a = R_c = 3\ \mu\Omega$.

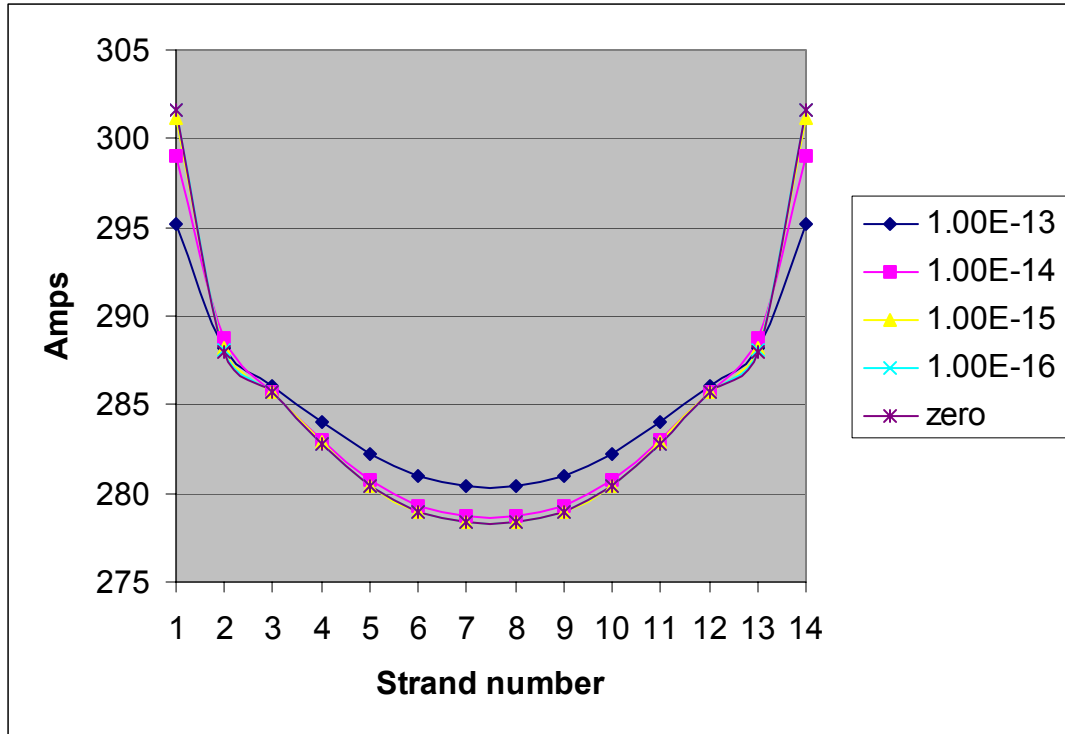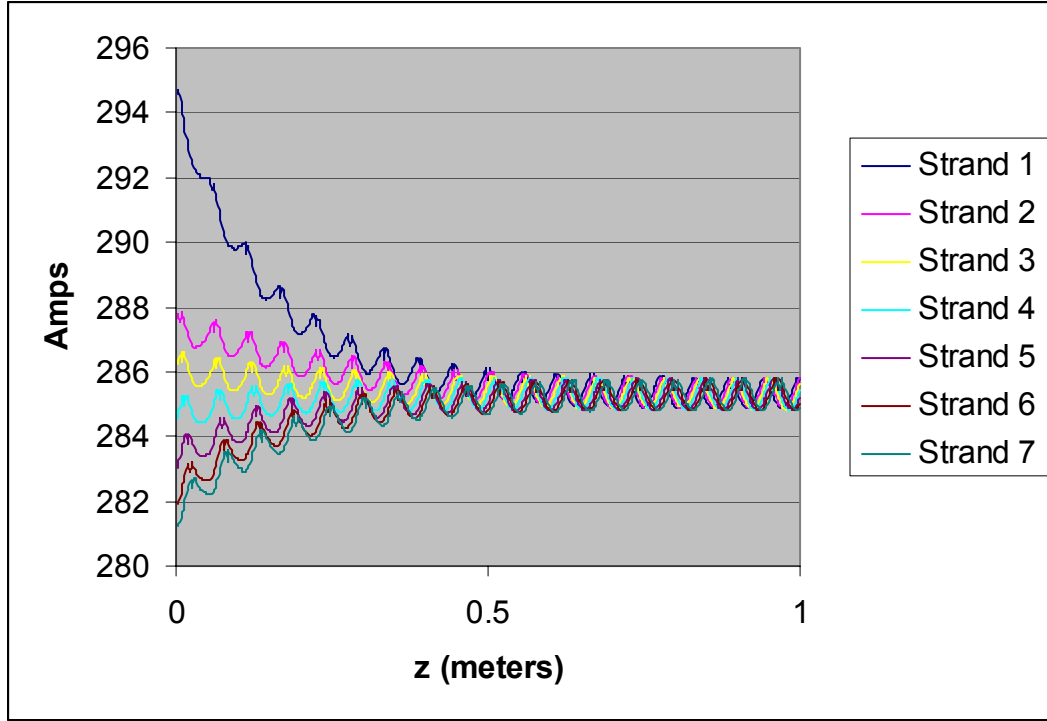Figure 6   The distribution of strand currents, at the crossection $z = 0$, for five different values of ρ_s. The values used for the other parameters were: $d_s = 1 \ mm$, $R_a = R_c = 3 \ \mu\Omega$, and ramprate = 400 Amps / sec. The expected value of strand current (if there was no imbalance) at this instant of time is 285.7 Amps
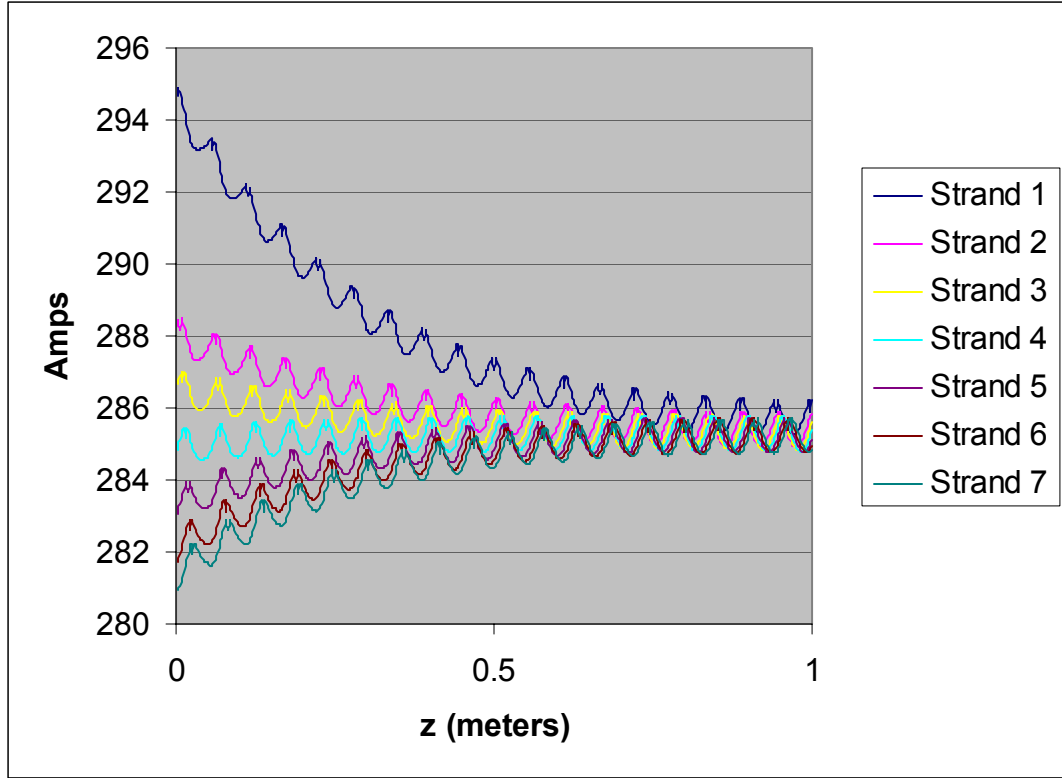
Figure 7   The distribution of strand currents along the cable length for a current
ramprate of 400 Amps / sec, $d_s = 1 \ mm$, $\rho_s = 10^{-13}\,\Omega\cdot m$, and
$R_a = R_c = 3 \ \mu\Omega$. The total length of the cable is $20L_p \approx 2 \ m$.

Figure 8   The distribution of strand currents along the cable length for a current ramprate of 400 Amps / sec, $d_s = 1\ mm$, $\rho_s = 10^{-14}\,\Omega \cdot m$, and $R_a = R_c = 3\ \mu\Omega$. The total length of the cable is $20L_p \approx 2\ m$.
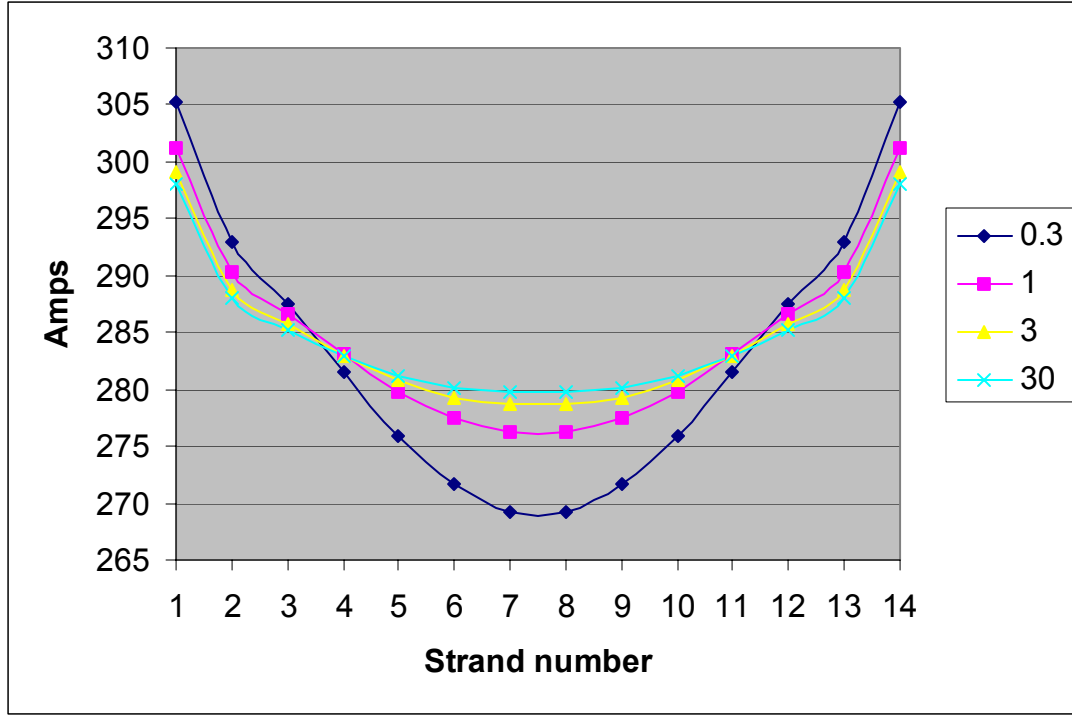
Figure 9   The distribution of strand currents, at the crossection $z = 0$, for four different values of contact resistance $R_a = R_c = 0.3,\ 1.0,\ 3.0,\ 30.0\,\mu\Omega$. The values used for the other parameters were: $d_s = 1\ mm$, $\rho_s = 10^{-14}\,\Omega \cdot m$, and ramprate = 400 Amps / sec. The expected value of strand current (if there was no imbalance) at this instant of time is 285.7 Amps
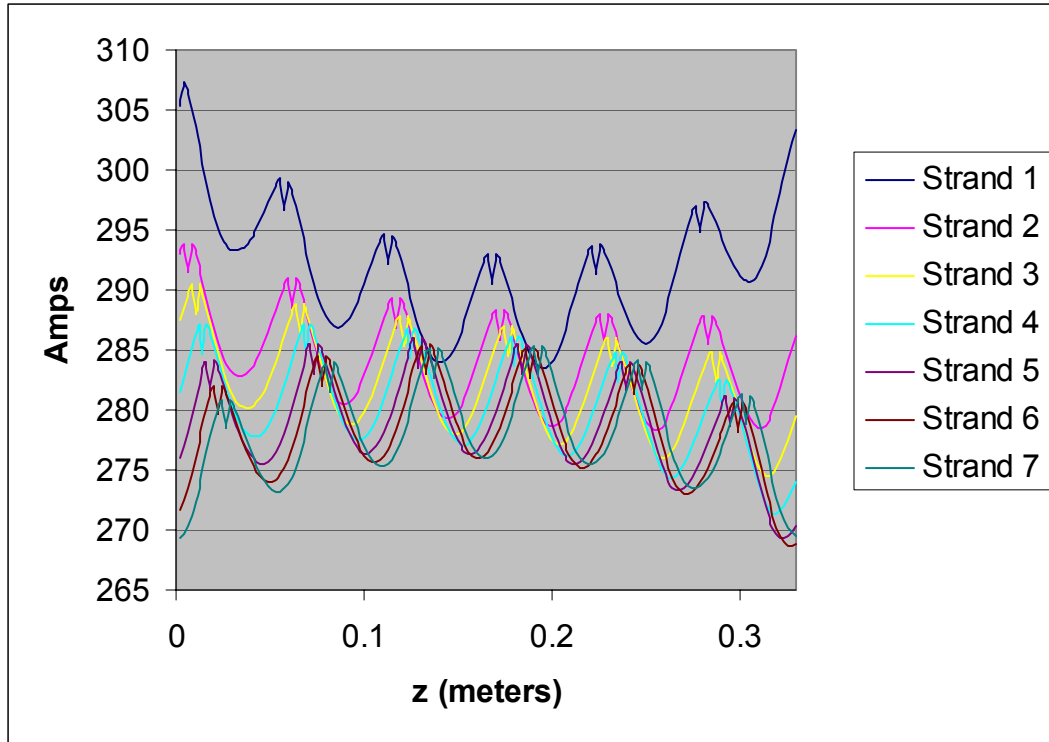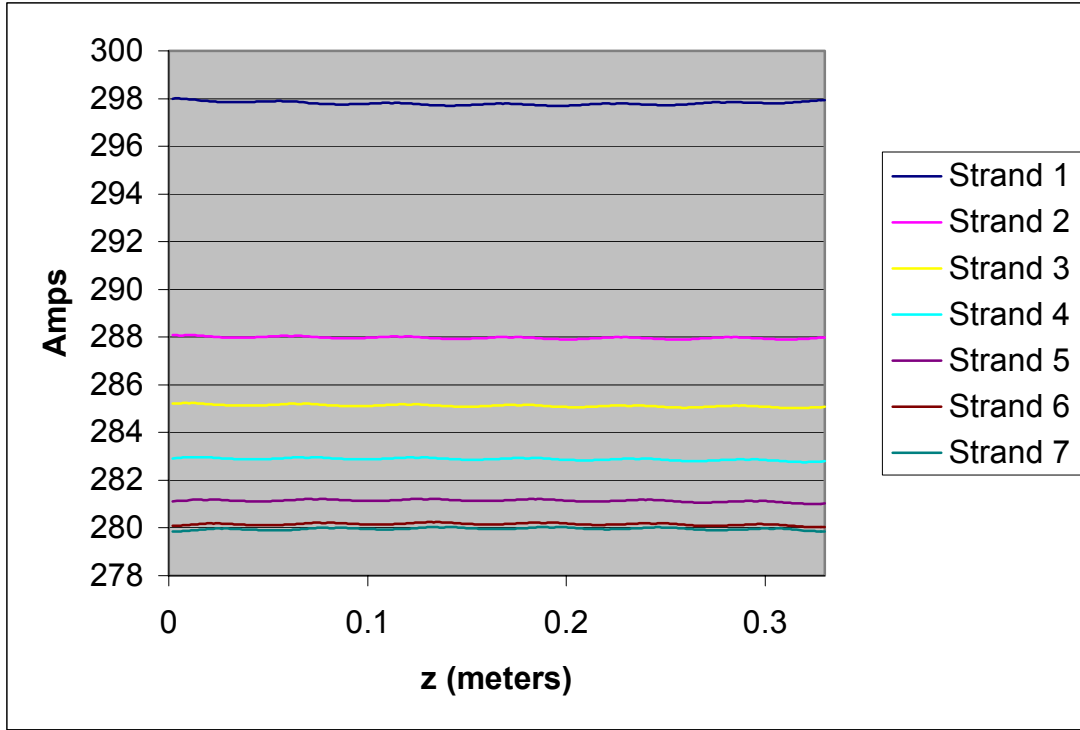
Figure 10   The distribution of strand currents along the cable length for a current
            ramprate of 400 Amps / sec, $d_s = 1\ mm$, $\rho_s = 10^{-14}\Omega \cdot m$, and
            $R_a = R_c = 0.3\ \mu\Omega$.

Figure 11   The distribution of strand currents along the cable length for a current
ramprate of 400 Amps / sec, $d_s = 1\ mm$, $\rho_s = 10^{-14}\,\Omega \cdot m$, and
$R_a = R_c = 30\ \mu\Omega$.

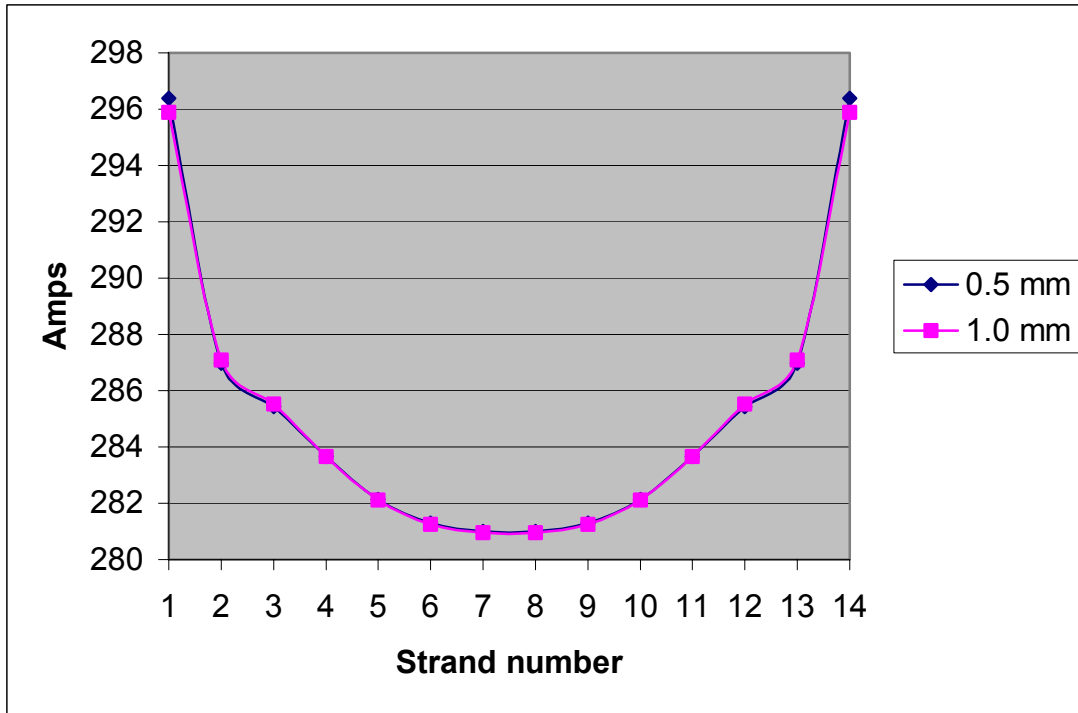Figure 12   The distribution of strand currents, at the crossection $z = 0$, for two
different values of strand diameter. The values used for the other
parameters were: $\rho_s = 0$, $R_a = R_c = 3$ $\mu\Omega$, and ramprate = 200 Amps /
sec. The expected value of strand current (if there was no imbalance) at
this instant of time is 285.7 Amps